Papers

A simple model of light transmission through the atmosphere over the Baltic Sea utilising satellite data*

OCEANOLOGIA, 50 (2), 2008.
pp. 125–146.

KEYWORDS
Solar energy
Baltic Sea
Satellite remote sensing

Adam Krężel*
Łukasz Kozłowski
Marcin Paszkuta

Institute of Oceanography,
University of Gdańsk,
al. Marszałka Piłsudskiego 46, PL–81–378 Gdynia, Poland;

e-mail: oceak@univ.gda.pl

*corresponding author

Received 22 November 2007, revised 6 May 2008, accepted 19 May 2008.

Abstract

A simple spectral model of solar energy input to the sea surface was extended to incorporate space-borne data. The extension involved finding a method of determining aerosol optical thickness (on the basis of AVHRR data) and the influence of cloudiness (on the basis of METEOSAT data) on the solar energy flux. The algorithm for satellite data assimilation involves the analysis of satellite images from the point of view of cloud identification and their classification with respect to light transmission. Solar energy input values measured at the Earth's surface by traditional methods were used to calibrate and validate the model. Preliminary evaluation of the results indicates a substantial improvement in the accuracy of

* The work is a part of a project supported by the Polish State Committee for Scientific Research (now the Ministry of Science and Higher Education) – grant No. PBZ–KBN 056/P04/2001.

estimates of solar energy input to the sea surface in relation to models utilising only traditionally obtained data on the state of the atmosphere.

1. Introduction

The dose of solar energy within the spectral range defined as photosynthetically active radiation (PAR) reaching the sea surface at a given time is one of the basic input parameters used in primary production models. Although this value is relatively easy to measure, it is practically impossible to do so in a sea area where it is difficult and expensive to put in place a sufficiently dense network of the necessary measurement apparatus. Indirect methods are therefore called for: these are based on the solution to the energy transfer equation enabling PAR to be determined with the necessary accuracy from atmospheric parameters measurable at a given instant at any site in a sea area under study. Suggested by numerous authors (e.g. Justus & Paris 1985, Bird & Riordan 1986, Laine et al. 1999, Gueymard 2001), these solutions were further developed in the present study for application to the Baltic Sea.

The basic problem in almost all of these solutions, however, is with the parameterisation of the effects of clouds and aerosols. Exerting a strong influence on light transmission through the atmosphere, both factors are highly variable in time and space. Moreover, there are no easily measurable values that can directly determine their contribution to the radiation balance at sea level.

The objective of the present study was to extend existing solutions, used to determine the influence of the above factors on light attenuation in the atmosphere, by making use of visible and near-infrared data recorded by spectrophotometers aboard environment-monitoring satellites. Since access to such data (also in operational mode) is relatively easy, it is suggested that AVHRR data be used, supplemented with cloudiness data recorded by METEOSAT and/or MSG geostationary satellites (at high scanning frequencies).

2. Material and methods

2.1. Material

Satellite-borne radiometers are practically the only source of information enabling the determination of cloudiness over the sea. In view of the desired sampling frequency, geostationary meteorological satellites producing an image of the Earth's surface every half hour (METEOSAT) and even every 15 minutes (MSG) were taken into consideration.

Because the study area lies in latitudes that are relatively high for measurements made from a geostationary orbit, only METEOSAT 7 visible channel data (rendered accessible in the digital format OPEN_MTP by EUMETSAT) were utilised. The size of every image was 5000×5000 pixels, where the pixel size in the undersatellite point was 2.5×2.5 km. Figure 1 presents an image from which the Baltic Sea area was cut out for further analysis.

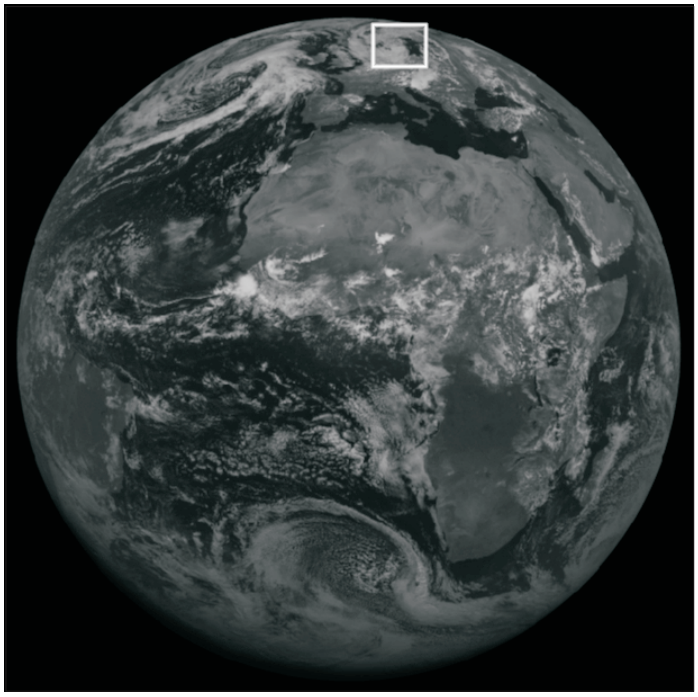

Figure 1. Model input data: Meteosat 7 image in the visible channel; the study area is marked

Afterwards, the radiance values recorded by the radiometer were used to calculate the albedo at the top of the Earth's atmosphere with the following formula:

$$A_s = L_s \frac{\pi}{E_{M_1} \cos \vartheta}, \tag{1}$$

where E_{M_1} – irradiance at the top of the atmosphere (690.80 W m^{-2} for METEOSAT 7 channel 1), ϑ – angle at which solar rays reach a given point at a given time, L_s – radiance recorded by the satellite (decoded) [W m^{-2} sr^{-1}], expressed as $L_s = C_f(t)(D_C - D_{C_0})$ and $C_f(t) = C_f + D_f N_t \times 10^{-5}$, D_C – coded value of the radiance, D_{C_0} – offset value taken from

calibration tables, $C_f(t)$ – calibration coefficient dependent on the sensor 'age', C_f – calibration coefficient determined prior to satellite launching (=0.9147), D_f – diurnal variability of the calibration coefficient (=5.7453 W m^{-2} sr^{-1} D_C^{-1} day^{-1}), N_t – number of days elapsed since the launching of METEOSAT 7 (2 October 1997).

In the next part of this analysis, a cut-out of a satellite image of the Earth's albedo in the OPEN_MTP format (Figure 1) was converted into a map using the UTM33N projection. The values in the new, regular grid were interpolated using the Nearest Neighbourhood Method. Then, the area of land was masked in such a way that further calculations applied only to the area of the sea (excluding islands as well). It could then be assumed that when the radiance recorded by the satellite-borne radiometer exceeded a threshold value, the reason for this was the state of the atmosphere reflecting the radiation rather than the variability of the land cover.

The results of this investigation (the values calculated using the method developed here, i.e. coefficients determining the cloud cover) were evaluated with the aid of data generated by the ICM[1] numerical weather prediction model and those recorded at the Institute of Oceanography's automatic measurement station at Hel. The modelled data included cloudiness, air pressure and water vapour pressure measurements, whereas in the case of the Hel station they were the irradiance data (across the whole spectrum and PAR range) recorded continuously during a single day. Calculations were carried out with the use of our own code and MicroImages Inc. TNT-MIPS version 7.0 software.

2.2. Methods

Light transmission through the atmosphere

It is assumed that the density flux of solar radiation energy (irradiance) reaching the sea surface within a given spectral band $\Delta\lambda$ can be presented in the following form:

$$E = \int_{\lambda_1}^{\lambda_2} [E_S(\lambda)\cos\vartheta + E_d(\lambda)]d\lambda T_{Cl}, \tag{2}$$

where E_s, E_d – sea surface irradiance due to direct solar radiation and radiation scattered in a cloudless atmosphere, respectively (Bird & Riordan 1986, Krężel 2001), ϑ – solar zenith distance, T_{Cl} – function defining

[1]Interdisciplinary Centre for Mathematical and Computational Modelling, Warsaw University, http://www.icm.edu.pl/eng/

the effect of cloudiness on irradiance transmission. Cloud transmission was assumed to be weakly dependent on wavelength (Barteneva et al. 1994). The quantity of direct solar radiation reaching the sea surface E_s depends on the number of interactions between the light and atmospheric components, and also on astronomical factors; this can be symbolically expressed as

$$E_s(\lambda) = \frac{F_s(\lambda)}{\beta^2} T_R(\lambda) T_{\mathrm{O}_3}(\lambda) T_G(\lambda) T_a(\lambda), \tag{3}$$

where F_s – spectral density of the solar constant, β – ratio of the mean to actual Sun–Earth distance, $T_R(\lambda)$ – transmission due to Rayleigh scattering, $T_{wv}(\lambda)$ – transmission due to the water vapour content in the atmosphere, $T_{\mathrm{O}_3}(\lambda)$ – transmission due to the ozone content in the atmosphere, $T_a(\lambda)$ – transmission due to aerosols, $T_G(\lambda)$ – transmission due to other significant components of the atmosphere.

With this formula, the irradiance level for a cloudless atmosphere can be determined and the influence of cloudiness taken into consideration separately. The algorithms enabling the determination of $T_R(\lambda)$, $T_{wv}(\lambda)$, $T_G(\lambda)$ and $E_d(\lambda)$ were defined after Bird & Riordan (1986) and Krężel (2001). The methods applied to calculate $T_{\mathrm{O}_3}(\lambda)$, $T_a(\lambda)$ and the cloudiness affecting the irradiance value at the Baltic Sea surface are described below.

Absorption by ozone

The influence of the ozone layer on solar radiation can be determined on the basis of following formula:

$$T_{\mathrm{O}_3}(\lambda) = \exp[-a_0(\lambda)\mathrm{O}_3 M_0], \tag{4}$$

where the relative optical mass of atmospheric ozone M_0 was defined after Iqbal (1983) as

$$M_0 = \frac{1 + \dfrac{h_0}{6370}}{\left(\cos^2\vartheta + \dfrac{2h_0}{6370}\right)^{0.5}} \tag{5}$$

and h_0 is the height of the maximum ozone concentration in the atmosphere, generally accepted as being 22 km. The absorption coefficients of ozone a_0 were introduced after Neckel & Labs (1981). The mean nine-year (1997–2005) O_3 values, defining ozone concentration in an atmospheric air column of unit base area, for latitudes 50°–60°N in individual months were used in the calculations (Table 1).

Table 1. Mean nine-years (1997–2005) ozone concentration in the atmosphere in latitudes 50°–60°N (TOMS 2007)

	January	February	March	April	May	June	July	August	September	October	November	December
O_3 [cm]	0.37	0.39	0.40	0.39	0.38	0.36	0.33	0.32	0.31	0.30	0.32	0.35

Attenuation by aerosols

The influence of aerosols on light transmission is assessed by determining the so-called aerosol optical thickness of the atmosphere (AOT). When data on the current state of the atmosphere are lacking, it can be assumed to a first approximation that light attenuation by aerosols within the spectral band under consideration is weakly dependent on the wavelength. The average seasonal values for the Baltic region AOT≡a, determined on the basis of the data given by Krężel (1985), can be calculated from the formula:

$$\tau_a = -\sec\bar{\vartheta}\ln\bar{T}_a, \tag{6}$$

where $\bar{T}_a$ – average seasonal light transmission through a cloudless atmosphere in the Baltic region resulting from the presence of aerosols, $\bar{\vartheta}$ – mean seasonal solar zenith angle. The results can then be applied in the further analysis.

It is further assumed that AVHRR data can be utilised. The upward radiance over a dark sea surface in the red and infrared bands depends primarily on the type and concentration of aerosols in the atmosphere. The amount of solar radiation backscattered by aerosols is proportional to the aerosol optical thickness τ_a and the phase function $P^A(\gamma)$. Light attenuation by marine aerosols is due mainly to scattering (i.e. the single scattering albedo $\omega = 1$). Hence, the dependence between the radiance measured by the satellite-borne radiometer and τ_a should also make allowance for the geometric configuration between the light source and the direction of observation. This means that $P^A(\gamma)$ has to be known in order to determine the value of τ_a (Stowe et al. 1997).

The results of investigations done hitherto indicate that the variability of $P^A(\gamma)$ in the case of backscattering is very much lower than that of τ_a; to a certain extent, moreover, it does not even depend on the type of aerosol (Stowe et al. 1997). Koepke & Quenzel (1979) showed that the variability of $P^A(\gamma)$ lies within a range of about ±25% (and with an optimal geometric configuration) can be reduced to ±4%, whereas τ_a can range even over one order of magnitude. Kaufman (1993) demonstrated the

feasibility of determining τ_a from single-spectral-channel reflectance data; according to this author, the dependence between τ_a and the path radiance is a universal one.

The standard algorithms for determining AOT from single spectral AVHRR channel (1 or 2) data, developed for NOAA/NESDIS (first -generation algorithm), enable the geometric configuration of the system to be found. Moreover, a correction is made for the actual distance between the Earth and the Sun, and the values are rescaled according to the 0.5 μm wavelength (the rescaling coefficient is 1.348). Additional parameters used as input data are: (i) the ocean albedo (Lambert's reflection coefficient), (ii) volumetric absorption and scattering coefficients, and (iii) the phase function $P^A(\gamma)$, which is determined on the basis of Mie's theory and is redefined for the aerosol particle model.

The values of AOT (500) calculated by means of the above algorithm are rendered accessible in a quasi-operational mode by NOAA/NESDIS.

Figure 2 exemplifies the distribution of the AOT of the atmosphere over the Baltic Sea region at a wavelength of 500 nm and determined on the basis of AVHRR/3 data (NOAA 16) recorded between 9 and 16 January 2003.

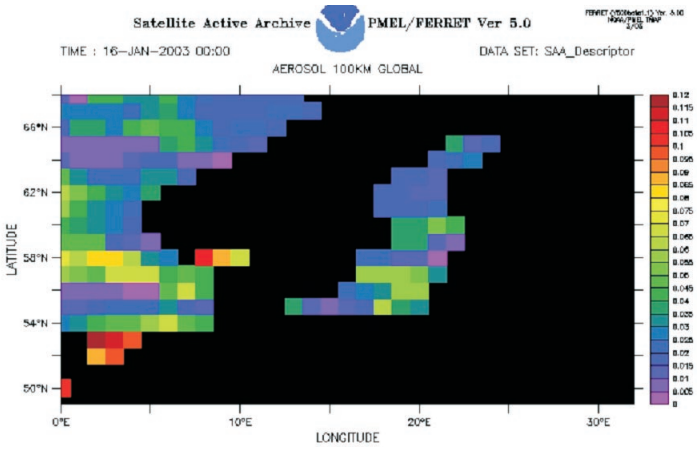

Figure 2. Aerosol optical thickness in the Baltic Sea region; AVHRR first-generation algorithm – http://www.class.noaa.gov/saa/products/

The use of AVHRR data in determining AOT enables its values to be obtained within a spectral interval of 100 nm with the central value at 630 nm. An algorithm enabling AOT variability to be determined within the whole visible spectrum was developed during this project (Rozwadowska

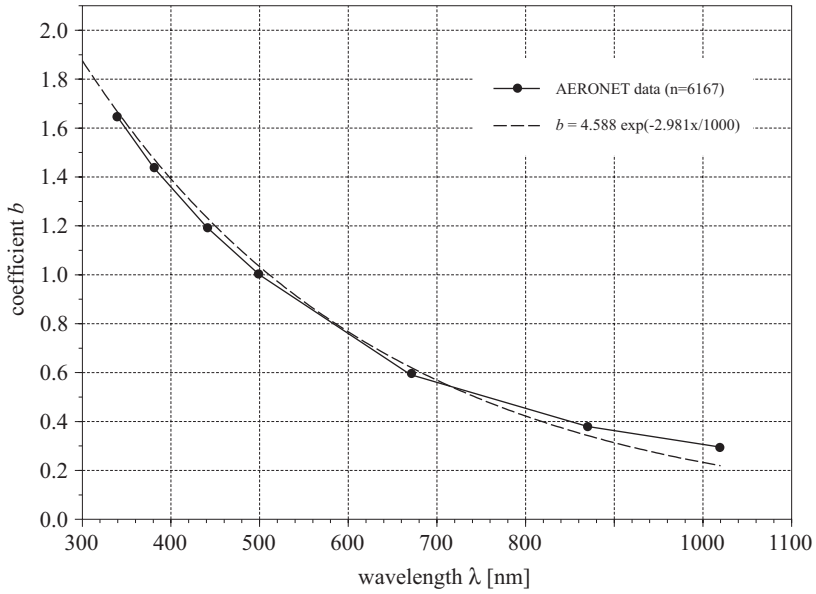

Figure 3. Values of $b(\lambda)$ in the Gotland area – for description, see text

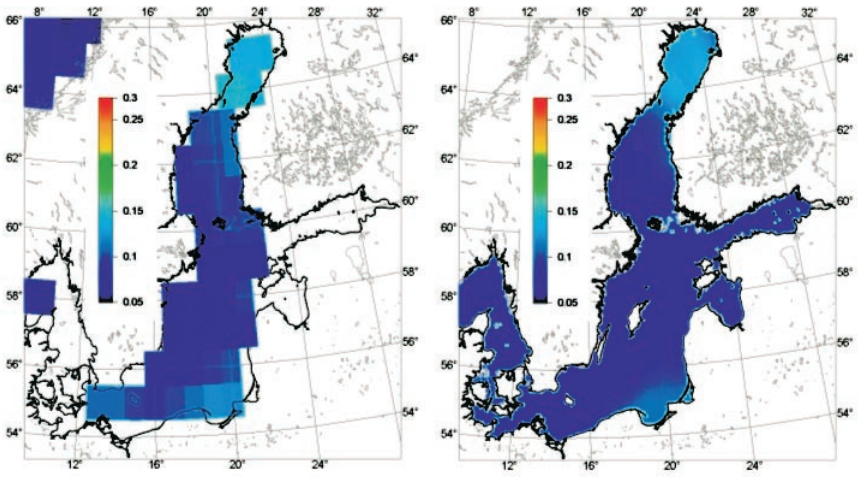

Figure 4. A map of aerosol optical thickness in the Baltic Sea region calculated on the basis of raw (a) and interpolated (b) AVHRR channel 1 data

et al. 2003). Based on the analysis of measurement data recorded mainly on Gotland (Figure 3) within the framework of the AERONET[2] programme,

[2]Aerosol Robotic Network, http://aeronet.gsfc.nasa.gov/

functional relationships enabling AOT to be determined for any wavelength within the PAR band were obtained:

$$AOT(\lambda) = AOT(500)a \ \exp b(\lambda), \tag{7}$$

where $AOT(500)$ – aerosol optical thickness at 500 nm determined from AVHRR data by means of the first-generation algorithm, a – empirical coefficient, γ – wavelength [nm], $b(\gamma)$ – coefficient related to the wavelength γ, which can be described by following formula:

$$b(\lambda) = 4.588 \times \exp(-2.981\lambda/1000). \tag{8}$$

The coefficient a in the eq. (7) was 1.63.

Relationships (7) and (8) make it possible to obtain digital images of $\tau_a(\lambda)$, some of which are presented in Figure 4.

Cloudiness

The solution to the problem of the influence of cloudiness on the solar energy flux reaching the Earth/sea surface can be divided into two stages:

- an assessment needs to be made of whether or not the Sun was obstructed by clouds at a given place and time – faulty assessment may cause the cloudiness to be over- or underestimated by almost one order of magnitude;
- should the Sun be covered by clouds, the relevant properties of clouds have to be determined, and also the degree to which they affect the value of the relevant parameter – the correct solution to this problem improves the accuracy of estimation by several percent.

Previous studies (see e.g. Krężel 1985) showed that if (i) the differences arising from astronomical reasons are filtered, (ii) areas with direct reflection of solar radiation are omitted, and (iii) the time or place where the sea is covered with ice is not taken into consideration, then the only factor significantly affecting the radiance reaching a satellite-borne sensor is the degree of cloud cover over the area from which the signal recorded by the satellite is generated. Daytime imaging, a sea area located at latitudes similar to those of the Baltic Sea, and the application of a method that can be used in operational mode resulted in the selection of possibly the simplest satellite image recognition method (Kidder & Vonder Haar 1995); the threshold technique is undoubtedly one such method. The basic problem to solve here is to determine threshold values, i.e. values of the albedo under a cloudless sky and under a completely overcast one, and to decide how to analyse the intermediate cases. The difficulty arises from the fact that the threshold value is a function of many variables, i.e. the type of surface (land, sea and their variability), its physical properties (e.g. temperature,

humidity, concentration of some substances in the water etc.), current weather conditions (e.g. wind, fog) and the Sun-pixel-satellite geometric configuration. This problem was solved empirically in three steps:

- the map of the Earth surface albedo at the top of the atmosphere in the Baltic Sea region was determined from METEOSAT data (diffusive radiation was taken into account);
- the solar radiation flux within the 300–1000 nm spectral band was calculated for stations where the solar radiation at the sea surface could be measured on a continuous basis;
- it was assumed that in the model of solar energy input to the sea surface (Krężel 1997) the average energy flux can be expressed as:

$$E = E_0 T_{Cl}, \tag{9}$$

where E_0 – irradiance reaching the sea surface from a cloudless atmosphere; T_{Cl} – a function describing the influence of average cloudiness on light transmission, given by Krężel (1985):

$$T_{Cl} = 1 - a_{Cl} c - b_{Cl} c^2, \tag{10}$$

where c – cloudiness in tenths, a_{Cl} and b_{Cl} best-fit coefficients.

This assumption can be adopted only for a sufficiently long averaging period; if it is longer, the calculation error is likely to be smaller. The main reason for this that formulas (9) and (10) make no allowance for cloud transmittance. This problem can be partially solved by introducing another variable in place of c. It has been suggested that a cloudiness coefficient c_T be introduced; this is a function of the albedo determined from an analysis of METEOSAT visible channel data in formula (10). In a sea area, this albedo is lowest where the sky is cloudless and highest where a thick layer of clouds covers a whole pixel. Intermediate values depend mainly on the degree of cloud and/or fog cover of each pixel and, on a smaller scale, on the transmittance of clouds and fog. Theoretically, the value of the albedo determined from a satellite contains resultant information, i.e. the albedo has almost the same value when a pixel is 50% covered with a thick layer of opaque clouds and when it completely covered with clouds of 50% transmittance. In the former situation the cloudiness $c = 0.5$ and the cloudiness coefficient $c_T = 0.5$; in the latter case $c = 1$ and $c_T = 0.5$.

Replacing c in formulas (9) and (10) with c_T should improve the results significantly. Nevertheless, differences between calculated and measured instantaneous irradiances can still be expected, especially in the case of extreme values, because the coefficient c_T contains no information on light reflection from the edges of cumulus clouds or cloud layer thickness: when

the thickness exceeds a certain value, any further increase has no effect on the satellite-measured albedo. The decrease in the averaging period will result in greater differences between modelled and measured values.

On account of the introduction of a new variable, fresh values of the regression coefficients in eq. (10) were determined.

3. Results

Data recorded in July 2000 (368 METEOSAT channel 1 images and the corresponding calculations of the irradiance done with a model using the input data generated by the ICM meteorological model) were used to calculate the best-fit coefficients.

The function connecting $c_{_T}$ with the satellite albedo A_S was determined from an analysis which made allowance for the conditions under which the Earth's radiation was measured. The radiance coming from the sea and/or clouds and reaching a satellite is

$$L_S = T_S[(1 - c_{_T})L_W + c_{_T}L_{Cl}], \tag{11}$$

where L_S – radiance reaching a satellite, L_W – radiance leaving the water surface towards the satellite, L_{Cl} – radiance leaving clouds towards a satellite, T_S – radiance transmission on the path towards a satellite, $c_{_T}$ – cloudiness coefficient.

In the simplest case, i.e. assuming that $T_S = 1$, the cloud albedo $A_{Cl} =$ const and the water albedo $A_W =$ const, the cloudiness coefficient can be expressed as a linear function of the albedo:

$$c_{_T} = aA_S + b, \tag{12}$$

where $a = 1/A_{Cl} - A_W$ and $b = -A_W/A_{Cl} - A_W$, and $A_S = L_S/F_s$ – the Earth surface albedo at the satellite level, $A_W = L_W/F_s$, $A_{Cl} = L_{Cl}/F_s$.

If the problem were further complicated by allowing for the Sun-pixel-satellite geometric configuration, i.e. if it was assumed that $T_S = f(\vartheta_S)$ and if the direct reflection of solar radiation towards the satellite (Figure 5) were eliminated, one would obtain

$$c_{_T} = a(\vartheta_\star, \vartheta_S)A_S + b(\vartheta_\star), \tag{13}$$

where $a = \dfrac{1}{T_S(\vartheta_S)[A_{DCl}(\vartheta_\star) - A_{Dw}(\vartheta_\star)]}$, $b = \dfrac{A_{Dw}(\vartheta_\star)}{A_{DCl}(\vartheta_\star) - A_{Dw}(\vartheta_\star)}$ and $A_D = L_D/F_s$ – albedo, L_D – diffusive radiance of water and clouds (subscripts $_W$ and $_{Cl}$), respectively, ϑ_* – solar zenith angle, ϑ_S – satellite zenith angle.

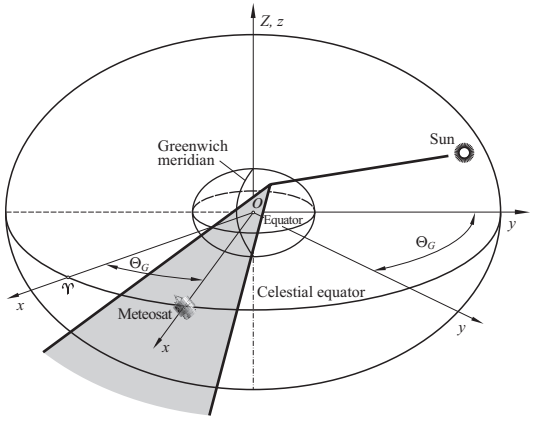

Figure 5. The satellite (METEOSAT)-pixel-Sun geometric configuration. The shaded area indicates the time interval eliminated from calculations (angle between the pixel-satellite direction and the direction of reflected solar rays); xyz – Celestial coordinate system, Υ – first point of Aries, θ_G – right ascension of METEOSAT

It is known that the sea surface albedo within the visible spectral band of the METEOSAT satellite also depends on the optical properties of the sea surface layer, that is, the albedo is higher when the water contains large concentrations of mineral suspended matter and lower when it is optically pure. On the other hand, for total cloud cover, when the concentration of water or ice particles forming the clouds exceeds a particular value, the light transmission through these clouds is very weak and is no longer related to their upper surface albedo. Hence, a relationship had to be found between the cloudiness coefficient and albedo determined on the basis of space-borne data and allowing for the above phenomena. It can be presented as a formula in which, apart from the value determined on the basis of satellite measurements (eq. (1)), variables are introduced relating to the maximum possible sea surface albedo g_l and minimum albedo of opaque clouds g_u above which the value of the solar energy flux reaching the sea surface changes negligibly:

$$c_T = \begin{cases} 0 & \text{for } A_S \le g_l(\vartheta_\star, \vartheta_S) \\ \dfrac{A_S - g_l(\vartheta_\star, \vartheta_S)}{g_u(\vartheta_\star, \vartheta_S) - g_l(\vartheta_\star, \vartheta_S)} & \text{for } g_l(\vartheta_\star, \vartheta_S) < A_S \le g_u(\vartheta_\star, \vartheta_S) \\ 1 & \text{for } A_S > g_u(\vartheta_\star, \vartheta_S). \end{cases} \tag{14}$$

The graphical representation of function eq. (14) is shown in Figure 6 (Model 1 (linear)), which also presents a graph of another function:

$$c_T = 0.5(1 + \tanh(0.027(b_h A_S - a_h))), \tag{15}$$

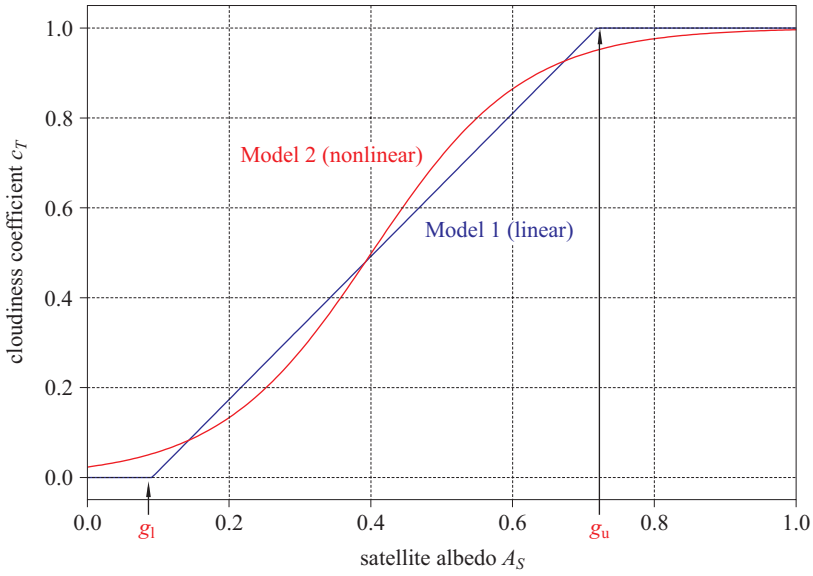

Figure 6. Relationship between the cloudiness coefficient and the satellite albedo determined on the basis of METEOSAT VIS channel data; g_l – maximum possible sea surface albedo, g_u – minimum albedo of opaque clouds

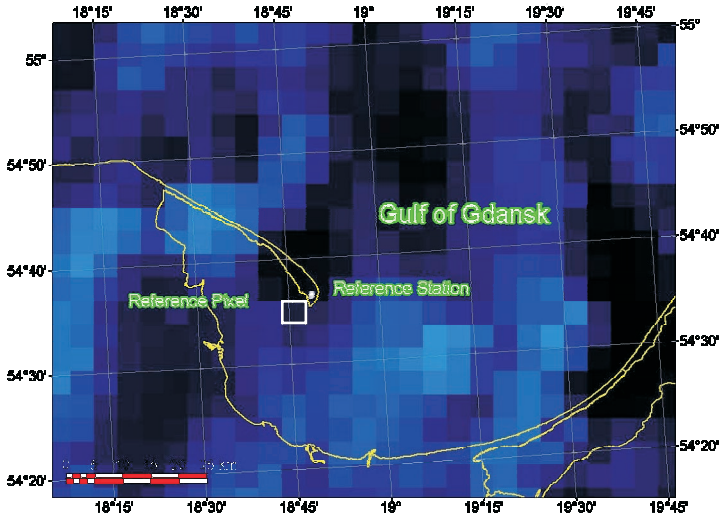

Figure 7. Location of the reference station and the area used to determine the factors in eq. (14)

where a_h, b_h – shape coefficients of a function that was also taken into consideration (Model 2 (non-linear)). A preliminary evaluation did not indicate any significant improvement in the investigated relationship when

the calculations were made more complicated; therefore, only formula (14) was used in the subsequent analyses. The non-linear Levenberg-Marquardt estimation was used to determine the best-fit coefficients in eq. (14). Two-minute average values of the downward irradiance measured at Hel were compared with the corresponding values calculated by the model and utilising METEOSAT data determined for a pixel whose central point was located about 3.5 km south-west of the reference station (Figure 7).

Calculations were carried out according to the frequency with which the upward radiance was recorded by METEOSAT, i.e. every 30 minutes during the hours of daylight ($\vartheta_\star < 90°$) from 1 July to 31 December 2004. Altogether, 3837 pairs of measured and calculated values were used.

The regression coefficients indicated that the influence of cloudiness on the atmospheric light transmission was considerably stronger than the values obtained from cloudiness data determined at meteorological stations in the traditional way (the solid line in Figure 8). Depending on the model, the difference was 20–30%. Cases where the angular distance between the satellite and the direction of reflected solar radiation (angle β_0) was smaller than 50° (points below the solid line in Figure 9) were discounted in the calculations so as to prevent signal gain due to the reflection of direct

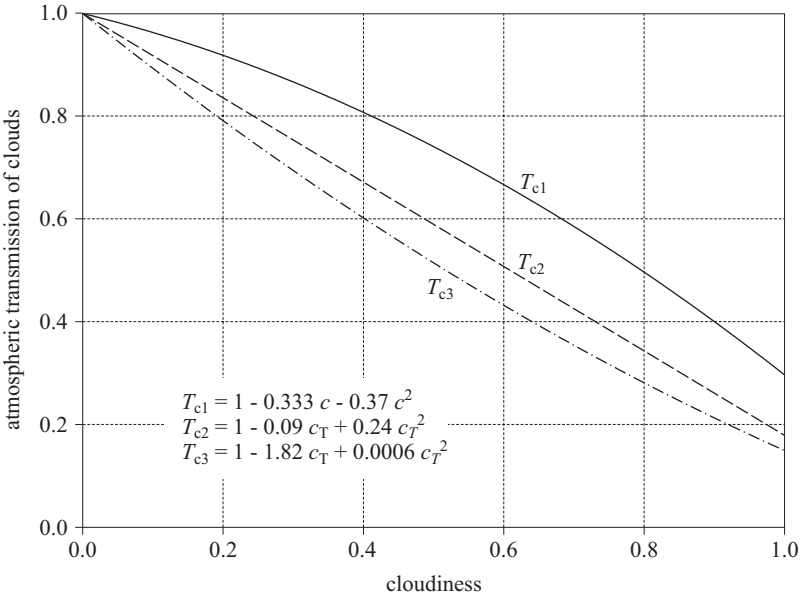

Figure 8. Atmospheric transmission as a function of cloudiness; T_{c1}, T_{c2} – present models; T_{Cl} – Krężel (1985)

solar radiation towards the satellite. As a result, the following formula was obtained:

$$c_T = \begin{cases} 0 & \text{for } A_S \leq 0.091 \\ \dfrac{A_S - 0.091}{(0.53 + 0.0027\vartheta_\star) - 0.091} & \text{for } 0.091 < A_S \leq 0.53 + 0.0027\vartheta_\star \\ 1 & \text{for } A_S > 0.53 + 0.0027\vartheta_\star. \end{cases} \quad (16)$$

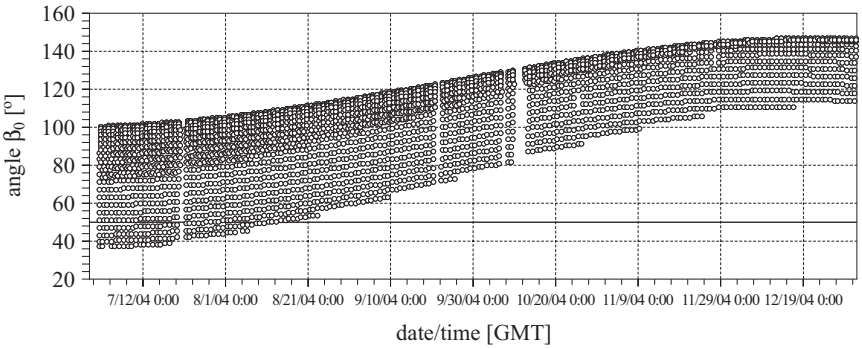

Figure 9. Values of the function β_0 for the Hel station during the second half of a year

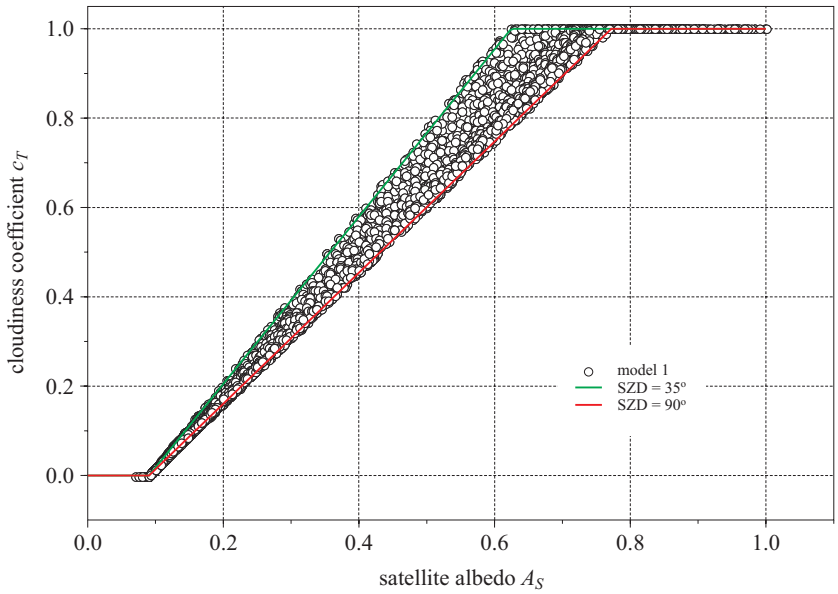

Figure 10. Determined dependency between the cloudiness coefficient and the satellite albedo (formula (14))

Regression analysis did not indicate any significant influence of the satellite zenith angle ϑ_S on the relationship or any dependence of the lower threshold value g_l on either the satellite or the solar zenith angles. Nevertheless, a relationship with the incident angle of the Sun's rays did exist. Figure 10 shows this dependence.

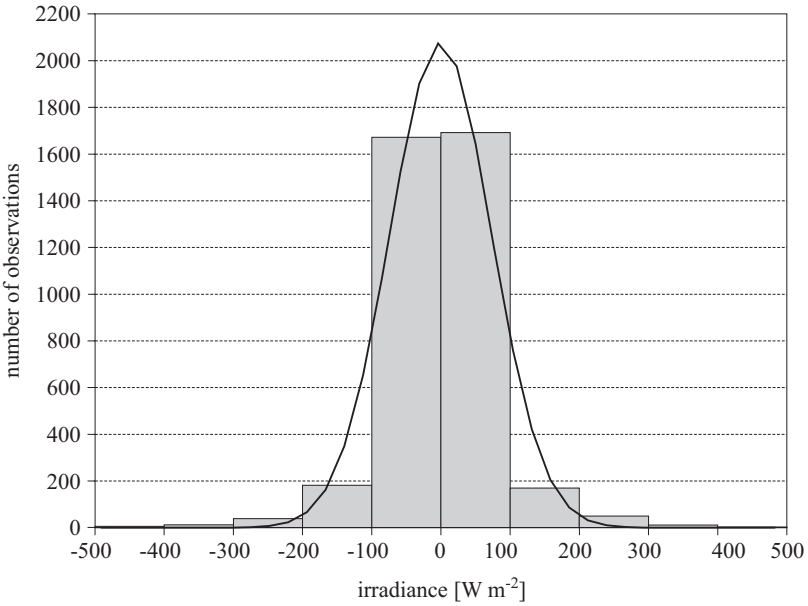

Figure 11. Histogram of the differences between measured and modelled irradiance values at Hel in the second half of 2004

Table 2. Comparison between some measured and modelled values

Period	Number of observations	Correlation coefficient	
		Model 1	Model 2
July 2004	861	0.914	0.912
August 2004	868	0.946	0.944
December 2004	403	0.881	0.883
all data	**3837**	**0.948**	**0.939**

The model was validated on the basis of actinometric measurements carried out at the Institute of Oceanography's Hel station. Figures 11 and 12 compare measurements and modelled values for the second half of 2004. These values appear to be in good agreement, which is confirmed by the correlation coefficients determined by way of example for three months

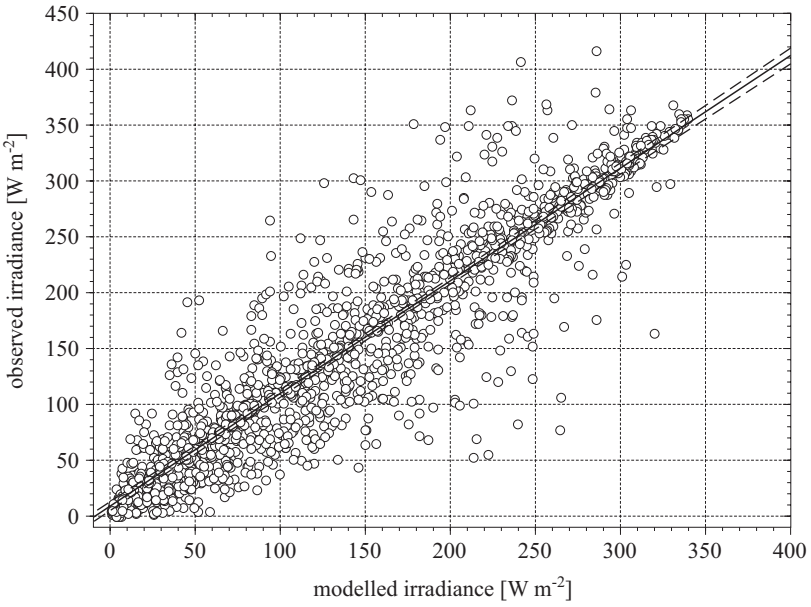

Figure 12. Observed and modelled values of PAR irradiance at Hel between 1 July and 31 December 2004

– July, August and December (Table 2). Nevertheless, the visible cloud and the values shown on the histogram (Figure 12) indicate that in individual cases the differences may be even more than 100%. Basically, this is because the compared values are instantaneous ones, and the most important factor affecting the irradiance, the cloudiness coefficient, was determined at a point lying some distance from the Hel measurement station (Figure 7). This hypothesis is confirmed by the irradiance variability series (Figure 13), in which time shifts of characteristic aspects of the curves are clearly in evidence. This effect was not apparent in periods when the Sun was not covered by clouds. In these situations the agreement between the two series is much better (e.g. this can be seen on 15 December 2004 in Figure 13).

The graph in Figure 14 is a good illustration of a feature typical of models, namely, the reduction of extreme values. As expected, modelled values under intermediate and slight cloud cover are often lower than measured ones. The reflection of solar radiation from the edges of cumulus clouds, which the model does not consider at all, may be one of the reasons for this. Another fact worth noting is the time lag between the measured and modelled values; this may be due to a disjunction between the time and place in which the parameter was measured and modelled. Moreover, spot measurements were compared with values spatially averaged over an area of about 25 km^2 (satellite data).

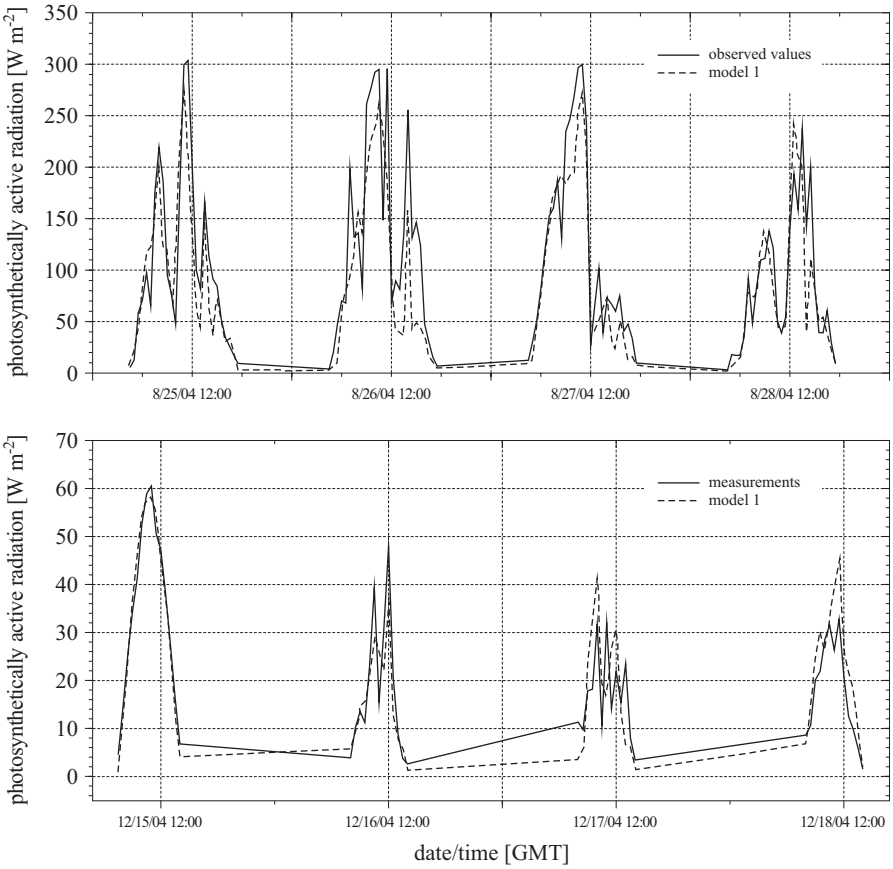

Figure 13. Examples of measured and modelled irradiance values

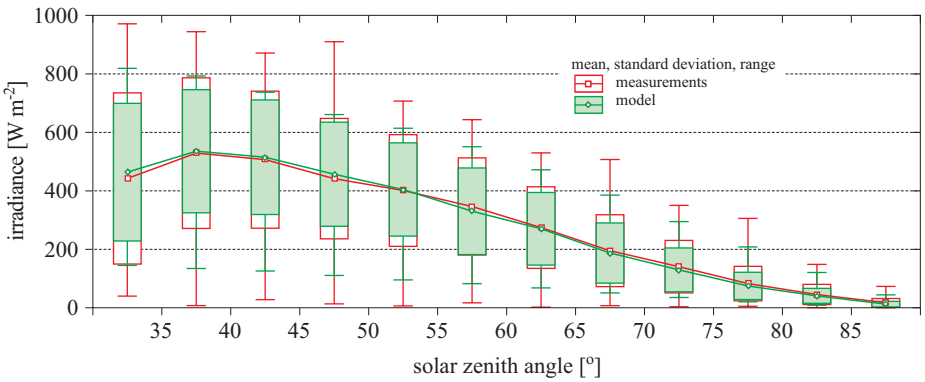

Figure 14. The PAR irradiance depending on the solar zenith angle at Hel in the second half of 2004

4. Conclusions

The model of light transmission through the atmosphere presented in this paper enables the magnitude of the solar energy flux at the sea surface

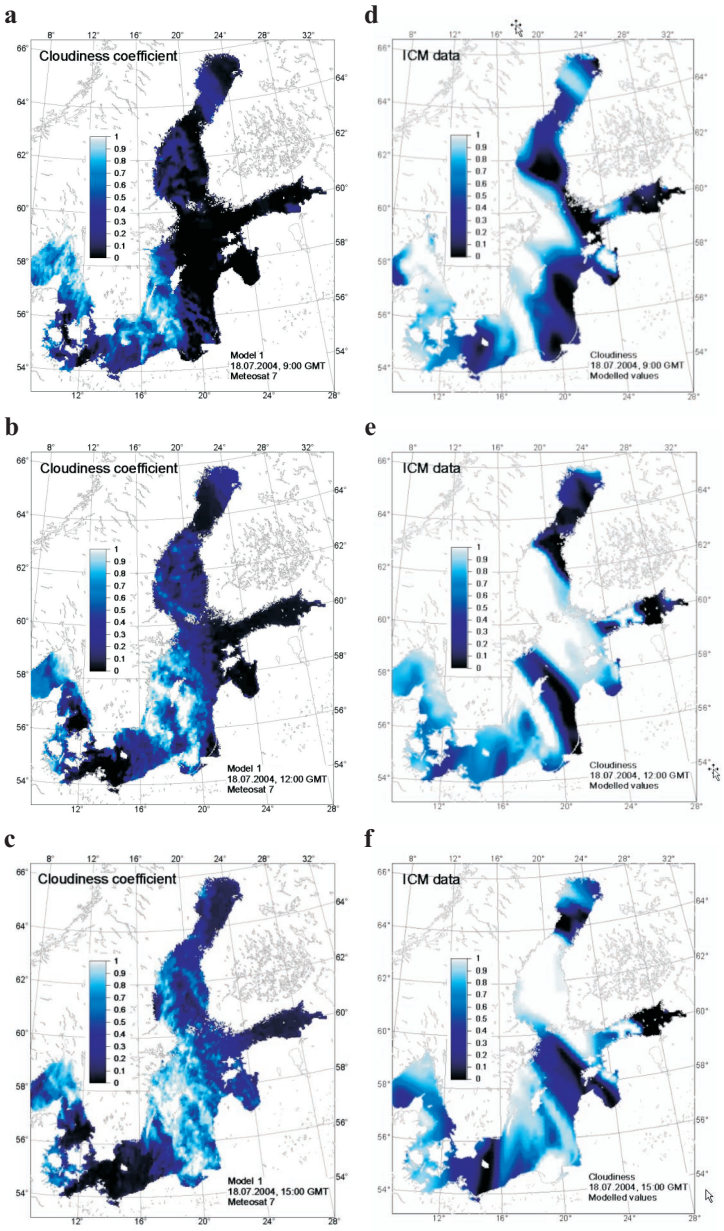

Figure 15. Distribution of cloudiness over the Baltic Sea determined on the basis of METEOSAT data and the ICM weather prediction model

to be determined for a cloudless atmosphere within any given spectral interval in the 300–1000 nm spectral range. It also permits satellite data on cloudiness and the influence of the aerosol on the magnitude of this flux to be used in calculations. Because of the large temporal variability in the case of cloudiness, it was assumed that data from the geostationary METEOSAT or MSG satellites could be utilised (data from the Tiros N/NOAA series satellites can also be used). It was further assumed that there is no spectral dependence of light transmission through clouds.

The influence of aerosols on the sea surface irradiance can be determined either on the basis of multiyear average aerosol optical thicknesses in the study area or by making use of AVHRR data. In the latter case the data are reproduced as an AOT spectrum on the basis of the data on radiation in the 630 nm region acquired by the analysis of the albedo in AVHRR channel 1 and/or 2 and AERONET data. Figures 15 and 16 compare cloudiness coefficients calculated for the Baltic Sea region with

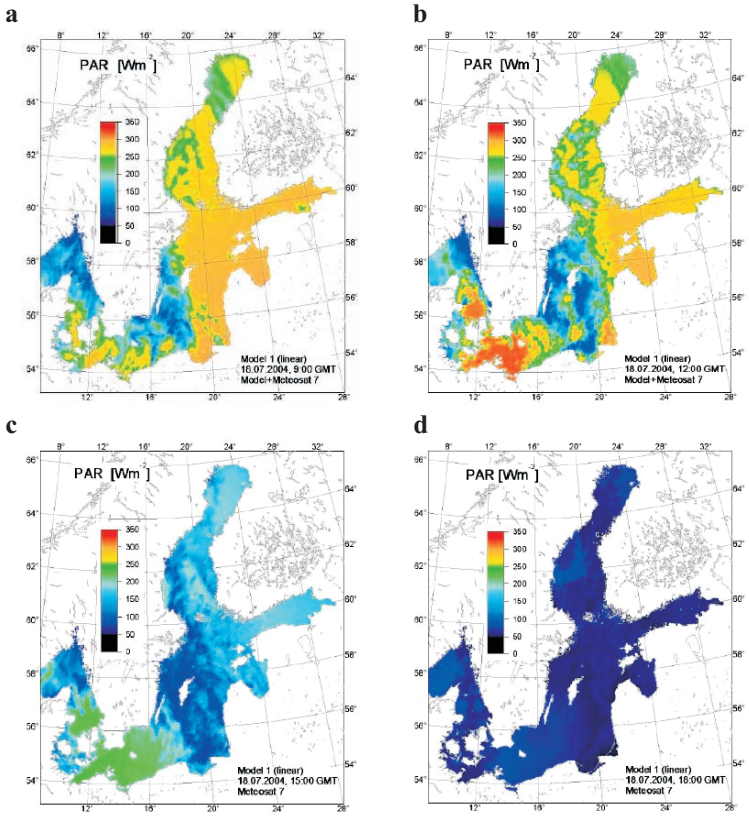

Figure 16. Diurnal variability of irradiation in the range of photosynthetically active radiation (PAR) at the sea surface determined using the model

values generated by the ICM numerical weather prediction model and values of the photosynthetically active radiation flux calculated using the model described in this article, which takes account of satellite data on cloudiness and AOT.

The use of satellite-borne information resulted in a considerably higher spatial variability of the cloudiness coefficient. It allows more reliable information to be obtained, and, even if the calculated light transmission by clouds is encumbered by a large error, the sea surface dose of solar radiation calculated with the use of this information will be closer to the actual value than the one obtained from information generated by the meteorological model.

The example shown in Figure 16 illustrates the possibilities of the model presented here. This generates such a map every half-hour between sunrise and sunset. The daily doses of PAR energy can be obtained by integrating this kind of information.

References

Barteneva O. D., Sakunov G. G., Timerev A. A., 1994, *Spectral transparency of upper-level clouds by ground based measurements in various climatic zones*, Atmos. Ocean. Phys., 30 (3), 362–367.

Bird R. E., Riordan C., 1986, *Simple solar spectral model for direct and diffuse irradiance on horizontal and tilted planes at the Earth's surface for cloudless atmospheres*, J. Appl. Meteorol., 25 (1), 87–97.

Gueymard C. A., 2001, *Parameterized transmittance model for direct beam and circumsolar spectral irradiance*, Sol. Energy, 71 (5), 325–346.

Iqbal M., 1983, *An introduction to solar radiation*, Acad. Press, New York, 390 pp.

Justus C. G., Paris M. V., 1985, *A model for solar spectral irradiance and radiance at the bottom and top of a cloudless atmosphere*, J. Appl. Mteorol., 24 (3), 193–205.

Kaufman Y., 1993, *Aerosol optical thickness and atmospheric path radiance*, J. Geophys. Res., 98 (D2), 2677–2692.

Kidder S. Q., Vonder Haar T. H., 1995, *Satellite meteorology: An introduction*, Acad. Press, San Diego, 466 pp.

Koepke P., Quenzel H., 1979, *Turbidity of the atmosphere determined from satellite: calculation of optimum viewing geometry*, J. Geophys. Res., 84 (C12), 7847–7856.

Krężel A., 1985, *Solar radiation at the Baltic Sea surface*, Oceanologia, 21, 5–32.

Krężel A., 1997, *Recognition of mesoscale hydrophysical anomalies in a shallow sea using broadband satellite remote sensing methods*, Diss. and monogr., Univ. Gd., Gdynia, 173 pp., (in Polish).

Krężel A., 2001, *Verification of the model of a solar energy radiation input to a sea surface against actinometric data*, Oceanol. Stud., 30 (3–4), 17–38.

Laine V., Venäläinen A., Heikinheimo M., Hyvärinen O., 1999, *Estimation of surface solar global radiation from NOA AVHRR data in high latitudes*, J. Appl. Meteorol., 38 (12), 1706–1719.

Neckel H., Labs D., 1981, *Improved data of solar spectral irradiance from 0.33 to 1.25 μm*, Sol. Phys., 74 (1), 231–249.

Rozwadowska A., Kozłowski Ł., Krężel A., 2003, *Parameterisation of optical properties of Baltic aerosols on the basis of AERONET data*, Report No. R35/03/UG of research funded by Polish State Committee for Scientific Research, grant No. PBZ-KBN 056/P04/2001, (in Polish).

Stowe L. L. Ignatov A. M., Singh R. R., 1997, *Development, validation, and potential enhancements to the second-generation operational aerosols product at the National Environment Satellite, Data, and Information Service of the National Oceanic and Atmospheric Administration*, J. Geophys. Res., 102 (D14), 16 923–16 934.

TOMS – Total Ozone Mapping Spectrometer, 2007, http://toms.gsfc.nasa.gov/ozone/ozoneother.html